

NIST Radiance Temperature and Infrared Spectral Radiance Scales at Near-Ambient Temperatures

S. N. Mekhontsev · V. B. Khromchenko ·
L. M. Hanssen

Published online: 18 April 2008
© United States Government Contribution 2008

Abstract The realization and the dissemination of spectral radiance and radiance temperature scales in the temperature range of -50 to 250°C and spectral range of $3\text{--}13\ \mu\text{m}$ at the National Institute of Standards and Technology are described. The scale is source-based and is established using a suite of blackbody radiation sources, the emissivity and temperature of which have been thoroughly investigated. The blackbody emissivity was measured using the complementary approaches of modeling, reflectometry, and the intercomparison of the spectral radiance of sources with different cavity geometries and coatings. Temperature measurements are based on platinum resistance thermometers and on the direct use of the phase transitions of pure metals. Secondary sources are calibrated using reference blackbody sources, a spectral comparator, a controlled-background plate, and a motion control system. Included experimental data on the performance of transfer standard blackbodies indicate the need for development of a recommended practice for their specification and evaluation. Introduced services help to establish a nationwide uniformity in metrology of near-ambient thermal emission sources, providing traceability in spatially and spectrally resolved radiance temperature, spectral radiance, and background-corrected effective emissivity.

S. N. Mekhontsev (✉) · L. M. Hanssen
Optical Technology Division (844), National Institute of Standards and Technology, 100 Bureau Drive,
Stop 8442, Gaithersburg, MD 20899-8442, USA
e-mail: snm@nist.gov

V. B. Khromchenko
Space Dynamics Laboratory, North Logan, UT 84341, USA

V. B. Khromchenko
Joint NIST/USU Program in Optical Sensor Calibration, North Logan, UT, USA

Keywords Blackbody · Effective emissivity · Infrared · Radiance temperature · Spectral radiance

1 Introduction

NIST has a well-established measurement history of spectral radiance and radiance temperature in the spectral range below $2.5\ \mu\text{m}$ [1,2], as well as several very successful developments in near-ambient thermal infrared (TIR) radiometry. The latter include a stirred water-bath blackbody [3] and a thermal infrared transfer radiometer [4] that remain “gold standards” for their particular application. However, thermal infrared measurements have remained non-spectral, with limited temperature coverage and large uncertainties at temperatures above 75°C [5].

At the same time, many applications depend on spectral radiance and radiance temperature of reference sources in the $3\text{--}5\ \mu\text{m}$ and $8\text{--}14\ \mu\text{m}$ ranges, including important remote-sensing applications [6], military infrared imagers, and electro-optical systems support tasks [7]. Emerging multi- and hyper-spectral imaging technologies employed for infrared signature discrimination are adding further demands for improved capabilities in the TIR.

A facility for direct measurements of spectral directional emissivity of materials [8], developed earlier in our group as part of the Fourier Transform Infrared Spectrophotometry Laboratory, has certain capabilities for spectral characterization of blackbody (BB) sources [9]. These capabilities, along with numerous excellent contributions from other groups [10–13], have allowed us to gain the necessary experience to proceed with establishment of a dedicated thermal IR spectroradiometric facility.

The main goal of this new facility, referred to as AIRI (Advanced Infrared Radiometry and Imaging), is to adequately meet current and emerging calibration requirements of transfer standard sources and radiometers in spectral radiance and spectrally resolved radiance temperatures across the temperature range from -50°C to $1,100^\circ\text{C}$ and the spectral range from $3\text{--}14\ \mu\text{m}$ and beyond.

This article will briefly describe all stages of spectral radiance and radiance temperature scale realizations and transfer. These stages include the development and characterization of primary standard blackbody sources, the design and construction of a spectral comparator and precision IR pyrometers, as well as the realization of, and validated methods, algorithms, and practices for, secondary standards calibration.

2 Realization—Approach, Tasks, and Results

2.1 Nomenclature

Before proceeding with the analysis, it is necessary to briefly discuss terminology, which is somewhat specific to the thermal IR due to the non-negligible ambient background and wide use of flat-plate sources, of which the emissivity can be reasonably well determined from reflectance measurements of the coating.

The most basic unit is “spectral radiance” L_λ , which is directly related to observable radiometric values. Most of the time we will use the term “apparent radiance”

L_{app} which is a superposition of “self-emitted radiance” L_{self} and “reflected background radiation” L_{refl} (which may include retro-reflected self-emitted radiance).

For temperature, we use “radiance temperature” T_{rad} (it is uniquely defined as the temperature of a perfect BB with radiance equal to the measured apparent radiance); the “nominal temperature” T_{nom} , which is fully equivalent to the “set-point temperature” T_{set} (referring to the control unit setting) or the “reference temperature” $T_{\text{reference}}$ (the latter used mostly in numeric modeling); and the “true temperature” T_{true} , which refers to the unknown temperature of the radiating surface.

Finally, for emissivity we use the “intrinsic emissivity” $\varepsilon_{\text{intr}}$, which is a property of the material and can be used only for flat-plate radiators along with the “true (surface) temperature” T_{true} ; the “apparent emissivity” ε_{app} , relating apparent radiance to that anticipated from a Planckian radiator at the nominal temperature; and the background-corrected “effective emissivity” ε_{eff} , which takes into account the reflected background term.

To illustrate the connection of these units, we can write the following exact relation:

$$\begin{aligned} L_{\text{app}}(\lambda, \theta, \varphi) &= Pl(T_{\text{rad}}, \lambda) = \varepsilon_{\text{app}}(\lambda, \theta, \varphi) Pl(T_{\text{nom}}, \lambda) \\ &= L_{\text{self}}(\lambda, \theta, \varphi) + L_{\text{refl}}(\lambda, \theta, \varphi) \end{aligned} \quad (1)$$

where Pl is the spectral radiance of a perfect blackbody at temperature T and wavelength λ in the environment with index of refraction n :

$$Pl(T, \lambda) = \frac{c_1 L}{n^2 \lambda^5 (\exp(c_2 / (n \lambda T)) - 1)} \quad (2)$$

Omitting for brevity the spectral index λ in directional emissivity and radiances, and assuming that the target is opaque, uniform, and has a Lambertian character of reflectance, we can re-write Eq. 1 as

$$L_{\text{app}} = \varepsilon_{\text{eff}} Pl(T_{\text{nom}}) + (1 - \varepsilon_{\text{eff}}) Pl(T_{\text{bg}}) = \varepsilon_{\text{intr}} Pl(T_{\text{true}}) + (1 - \varepsilon_{\text{intr}}) Pl(T_{\text{bg}}) \quad (3)$$

where T_{bg} is the temperature of the surrounding background radiation, which is assumed to be uniform, isotropic, and known.

2.2 Approach

Our scale realizations are source-based and illustrated in Fig. 1. The spectral radiance scale is derived from a set of blackbodies having overlapping temperature ranges, different principles of operation, and different cavity geometries. For each of the blackbodies, our best efforts have been made to determine their effective emissivity and temperature. As shown in Fig. 1, the effective emissivity of each cavity is determined in three independent ways. The first is based on reflectometric measurements (as reported at this conference [14]); the values obtained as summarized in Table 1 are found to be very close to the design targets as well as to the prediction of Monte

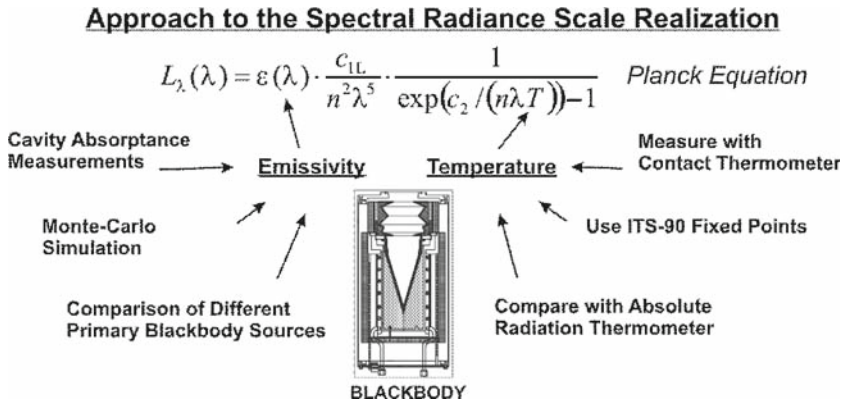


Fig. 1 Selected approach to realization of the spectral radiance scale

Table 1 Summary of blackbody cavity emissivity values inferred from total integrated scatter measurements with 1.32- μm and 10.6- μm lasers

Cavity	Emissivity (1-Reflectance)		Geometry (diameter, mm)	
	at 1.32 μm	at 10.6 μm	Cavity opening	Measured across
Water bath BB (Z302)	No data	0.99998	38	32
	No data	0.99995	38	28
Water heat-pipe BB (Nextel 3M)	No data	0.99988	38	28
Ga FP BB (Z302)	0.99991	0.99995	43	20
In, Sn FP BB (Graphite)	0.99972	0.99956	7	6

Carlo [15] modeling, our second method. Finally, we have validated these emissivity values by comparing independent primary sources, as shown later in this article.

Our temperature measurements are based on independent derivations of the ITS-90 temperature scale from contact thermometers and fixed-point BBs. It is anticipated that when the detector-based uncertainties of the IR pyrometer calibration approach the uncertainties of ITS-90 for the temperature range of interest, spectral radiance and temperature scales will become based on a thermodynamic temperature scale traceable to NIST cryogenic radiometers.

2.3 Realization Components

The primary components involved in the scale realizations are shown in Fig. 2, along with some relevant technical details. They include two groups of blackbody sources, namely fixed-point and variable-temperature BBs, and optical comparators, which are used to establish consistency of the temperature scale across the spectral range of interest and the overlapping temperature ranges of operation of the blackbodies. Figure 3 shows a photograph of the low-temperature cluster (LTC) of the AIRI facility, containing most of the aforementioned components.

The fixed-point blackbodies, all of which were designed, built, and characterized at NIST, operate at Ga (29.765°C), In (156.599°C), and Sn (231.928°C) fixed-point

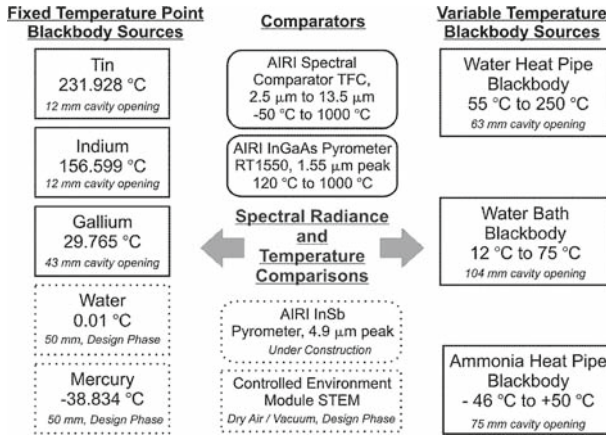


Fig. 2 Existing (solid boxes) and anticipated (dashed boxes) ARI components employed in the radiance temperature and spectral radiance scales realization

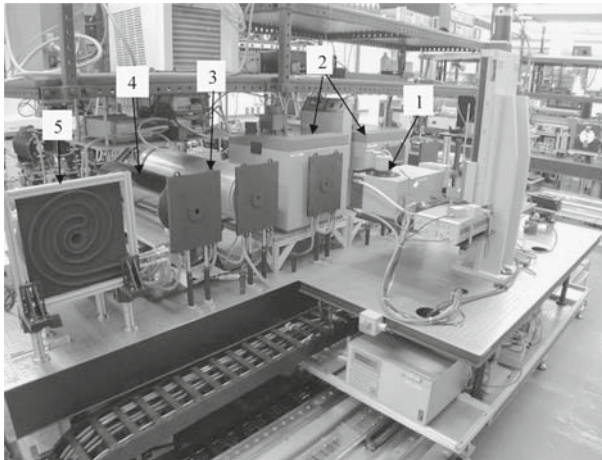


Fig. 3 Low-temperature cluster of the ARI Facility: 1—tunable filter comparator, 2—water-bath blackbodies, 3—water heat-pipe blackbody, 4—ammonia heat-pipe blackbody, 5—controlled-background plate

temperatures, while H_2O (0.01°C) and Hg (-38.834°C) are being considered as possible additions. Results of the detailed characterization of a large-aperture (37-mm useful diameter) Ga fixed-point BB are presented in another paper [16] at this conference. In and Sn blackbodies have 7-mm diameter exit apertures and are designed to have high IR emissivity and plateaux of several hours duration to allow long measurement times. Further details of their design and additional evaluations are described in an earlier paper [8].

The variable-temperature blackbodies include a water heat-pipe BB ($55\text{--}250^\circ\text{C}$) and two water-bath BBs [3] ($12\text{--}75^\circ\text{C}$) using a stirred water bath, all built at NIST, while an ammonia heat-pipe blackbody (temperature: -46 to 50°C) was built by IKE Stuttgart [17] in a manner similar to the one operating at NPL [18]. The results of a detailed characterization of the water heat-pipe BB are presented in a

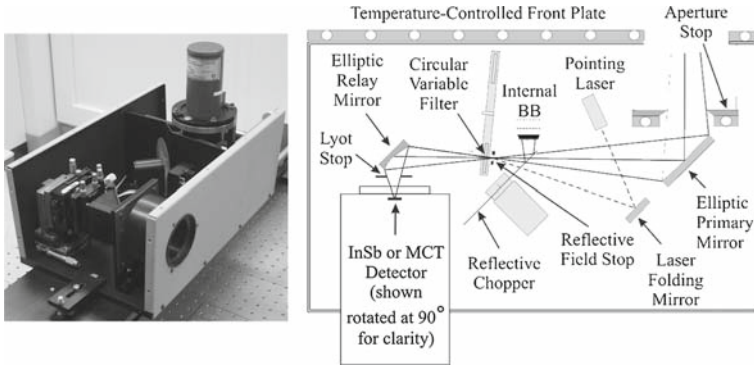


Fig. 4 AIRI tunable-filter comparator TFC

separate paper [19] at this conference. All variable-temperature BBs employ platinum resistance thermometers (PRTs) for their temperature determination.

For comparison of the primary standard blackbodies, AIRI uses a NIST-designed tunable-filter comparator (TFC), covering the spectral range from 2.5–13.5 μm, and a short-wave IR pyrometer RT1550 (1.55 μm peak, useful above 120°C), also designed and built at NIST. An addition of another pyrometer operating at 4.7 μm is anticipated in the near future.

The internal view and optical system of the TFC is shown schematically in Fig. 4. It incorporates a temperature-controlled front plate and aperture stop, an elliptical primary mirror, a reflective chopper with an actively stabilized internal reference source, a reflective field stop, a circular variable filter (CVF) mounted on a rotation stage, an elliptic relay mirror, and an LN₂-cooled InSb/MCT sandwich detector.

The TFC operates as a comparator, performing radiance interpolation between two reference blackbodies (“A” and “C”) to calculate the spectral radiance and radiance temperature of a unit-under-test (UUT). The TFC measurement sequence follows a pattern: A—UUT—C—UUT—A, which may be repeated, but the radiance of interest is calculated after each measurement cycle to reduce drift effects. In this case, this technique only requires short-term stability of the TFC during one cycle of the measurements.

Equation 4 shows how the spectral radiance L_{UUT} is calculated from the measured spectra and known radiances of the reference blackbodies:

$$L_{\text{uut}}(\lambda) = \left[\frac{[V_{\text{uut}}(\lambda) - V_A(\lambda)]}{[V_C(\lambda) - V_A(\lambda)]} \right] [L_C(\lambda) - L_A(\lambda)] + L_A(\lambda) \quad (4)$$

where V_A , V_C , and V_{UUT} are the measured spectra; L_A and L_C are the known spectral radiances of reference BBs A and C; and L_{UUT} is the spectral radiance of the customer BB.

The actual algorithm that is used is slightly more complicated because it takes into account the spectral shape of the CVF instead of assuming a single wavelength for each data point. The spectral transmittance of the CVF was separately measured at

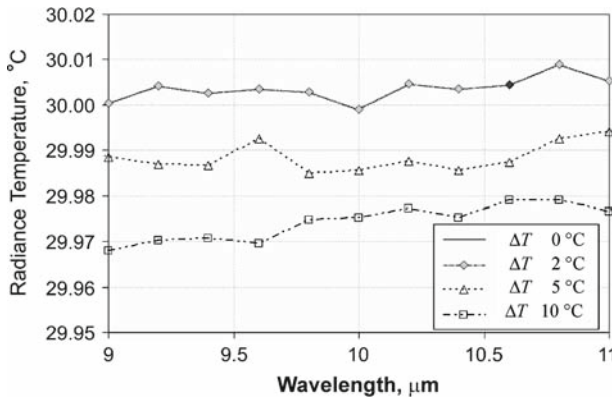
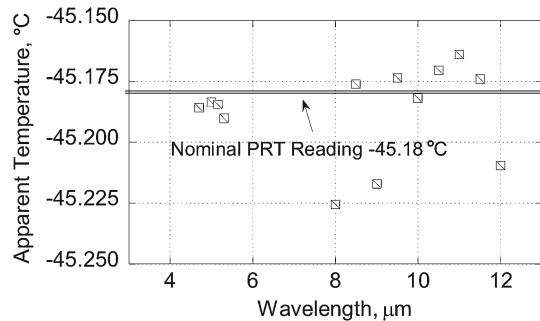


Fig. 5 Evaluation of spectral comparator uncertainty due to spectral mismatch and detector non-linearity by measuring the same blackbody with variable offset of the reference blackbody temperature. Contact temperature sensor reading of the source under test is 30.08°C

Fig. 6 Random uncertainty evaluation for TFC comparator, measuring ammonia BB at -45.18°C relative to itself and to a water bath BB at 11°C (auto-referencing measurement)



multiple wavelength settings. Figure 5 shows the typical sensitivity of the temperature interpolation process to differences between the unknown blackbody temperature and the nearest reference source. In this particular case, BB A had a constant temperature of 13°C , the unknown BB had a temperature of 30.08°C , and BB B had temperatures 30, 32, 35, and 40°C . In further experiments, we minimized the uncertainty of the interpolation by keeping the temperature difference between the unknown BB and one of the reference BBs within $1\text{--}2^{\circ}\text{C}$.

Another result that demonstrates the usable temperature range of the instrument is shown in Fig. 6, where the ammonia heat-pipe BB at a temperature set point of -45.18°C was measured using a room-temperature source and itself as references. The conclusion in this case is that the random uncertainty of the BB comparison at -50°C does not exceed 0.05°C both around $5\mu\text{m}$ and across the $8\text{--}12\mu\text{m}$ band. Further details of the TFC operation and characterization, including its temperature resolution, and spectral and spatial stray light measurement results, are beyond the scope of this article and will be covered in a forthcoming publication.

The transfer standard pyrometer, designated RT1550, with a spectral responsivity peaked at 1550nm , is used to interpolate the temperature scale between calibration points obtained using reference blackbody sources starting at 120°C . The pyrometer's

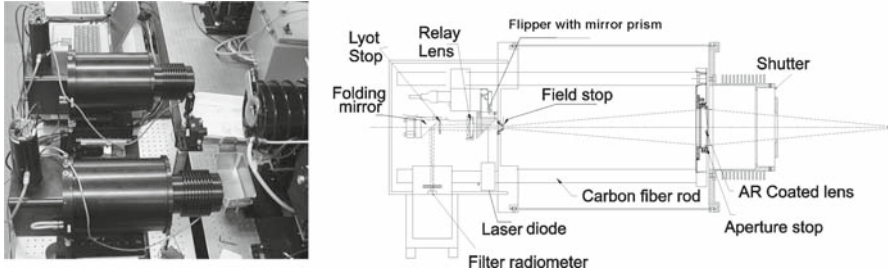
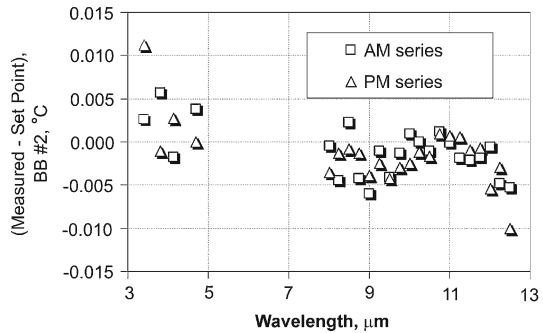


Fig. 7 AIRI reference radiation thermometer RT1550, peak wavelength of 1550 nm

Fig. 8 Results of measurements of radiance temperature of water bath #2 obtained using water bath #1 as a standard. Shown is a difference between measured (radiance) and set-point (PRT) temperatures



optical schematic and external view are shown in Fig. 7, while details of its design and evaluation can be found elsewhere [20].

The measurement setup is not purged. Hence, spectral comparison results are shown only for the ranges 3.4–4.2 μm, 4.4–5.4 μm, and 8–13.5 μm, outside the atmospheric absorption regions.

2.4 Results

Two stirred water-bath blackbodies WBBB#1 and WBBB#2, covering the central part of the temperature range of interest, have the smallest uncertainties and the best stability and uniformity. Figures 8 and 9 depict results of characterization of WBBB#1 and WBBB#2. Figure 8 demonstrates the level of agreement of blackbodies (the graph shows differences between measured radiometric and contact temperatures of the cavity). Figure 9 shows the typical spatial uniformity of the blackbody radiance temperature across the exit aperture. Results of a comparison of a WBBB with the Ga BB are presented in another paper [16].

The ammonia heat-pipe BB was compared with a WBBB in the temperature overlap region. Results of its radiance temperature measurements using the WBBB as a reference are shown in Fig. 10, and agreement with the anticipated temperature is within 0.025°C. So far, we have no means to independently validate the ammonia heat-pipe BB temperature uncertainty below 10°C other than by comparisons with

Fig. 9 Vertical and horizontal spatial uniformity of water bath radiance temperature at $10\ \mu\text{m}$. Reference PRT reading is 56.206°C

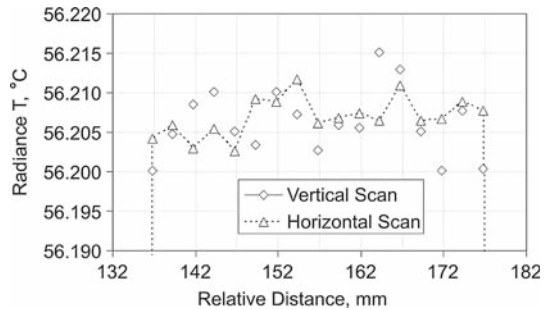


Fig. 10 Spectrally resolved radiance temperature of the ammonia HP BB, measured relative to the water-bath blackbodies. Reference PRT reading is 30.06°C

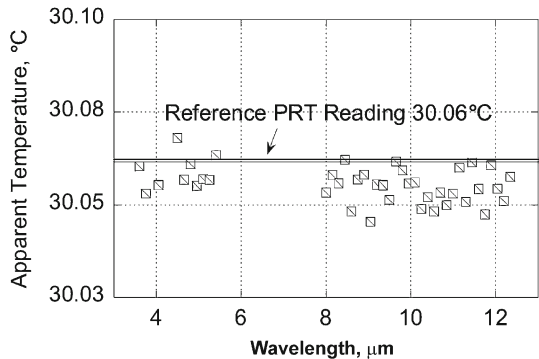
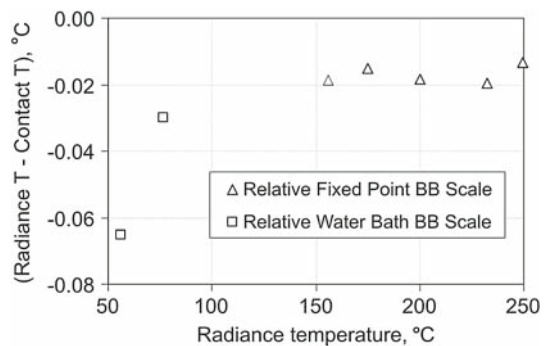


Fig. 11 Comparison of water HP BB radiance temperature with reference PRT readings. Shown is the difference between measured radiance temperature and contact (PRT) temperature



another national laboratory, but most of these laboratories rely on nearly identical ammonia heat-pipe BBs, which may leave some systematic uncertainties unnoticed.

The water heat-pipe blackbody (water HP BB) was compared with both a WBBB (in the temperature overlap region from $55\text{--}75^\circ\text{C}$) using the TFC comparator, and with In and Sn fixed-point BBs by means of the RT1550 pyrometer. Figure 11 shows the results of the comparison of the water HP BB reference PRT with the radiance temperature scales. Further results of this BB characterization can be found in a separate paper [19].

3 Dissemination—Approach, Tasks, and Results

3.1 Approach and Instrumentation

Dissemination of the radiance temperature and spectral radiance scales can be realized by the calibration of customer sources, pyrometers, and imaging systems. The task of interpolation over the temperature range, maintenance, and dissemination of the radiance temperature scale relies on variable-temperature BBs. Calibration of pyrometers in the AIRI facility is performed directly by pointing the pyrometers at the reference sources operating at the temperature of interest. To provide identical background conditions and source size during pyrometer calibration, all sources are fitted with temperature-stabilized aperture plates with variable-size inserts, with a maximum opening of 50 mm diameter. To allow the customer to estimate an application scene-specific uncertainty due to spatial scatter of the pyrometer, size-of-source (SSE) measurements are performed using an extended temperature-controlled plate. The exposed diameter of the plates can be varied from 12–500 mm. A detailed description of the apparatus and methods involved can be found in a separate paper [21].

Many of the thermal IR applications rely on flat-plate blackbodies, the design of which makes them especially sensitive to imperfect surface emissivity, radiance temperature non-uniformity, and varying ambient conditions. In the meantime, claims of their manufacturers cannot be verified without appropriate standards. Characterization of such sources requires special emphasis on (a) a controlled-background radiation environment, (b) the capability to handle large amounts of scattered light originating from a radiating area with typical sizes up to 300 mm × 300 mm, and (c) spatial mapping capabilities. AIRI was designed specifically to meet these needs. Figure 12 is a schematic diagram of the spectral calibration of our customer BB sources. Along with reference and customer blackbodies and a comparator, the setup contains a controlled-background plate (CBP), similar to the one described previously and successfully used at CSIRO by Ballico [10]. This component is essentially a sandwich of two

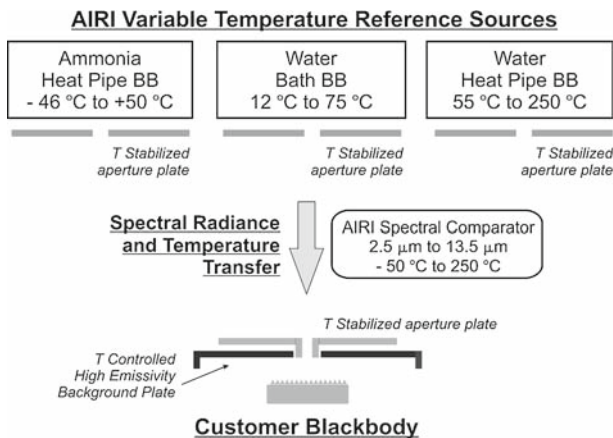


Fig. 12 Radiance temperature and spectral radiance scales dissemination schematic

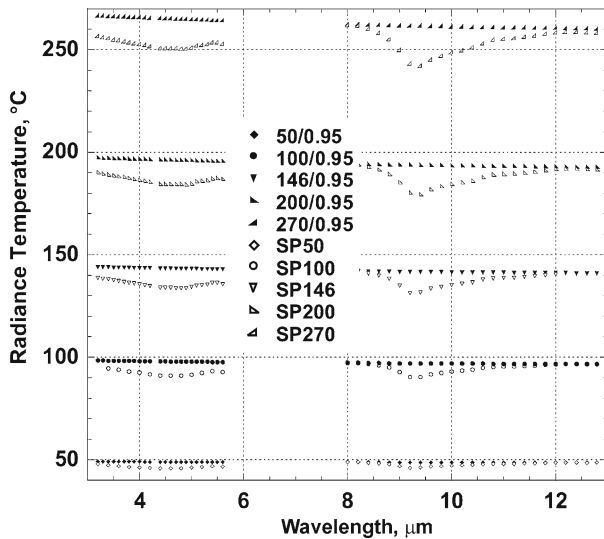


Fig. 13 Expected and actual radiance temperature of a high-temperature flat-plate blackbody. Light symbols denote anticipated radiance temperature calculated using set-point (SP) temperature, nominal emissivity of 0.95, and background temperature of 24°C. Filled symbols denote measured values

black plates with temperatures that are independently controlled. Knowledge of the radiation background temperature enables one to deduce the customer blackbody's effective emissivity from Eq. 3 and experimentally defined apparent spectral radiance of the UUT. We are currently in the process of evaluating the CBP uncertainty for selective and low-emissivity targets. Until this study is completed, only targets with an emissivity above 0.8 can be calibrated with a well-defined uncertainty.

Characterization of a UUT involves the following operations for each set point of interest: (a) a uniformity scan (linear or full map) at a selected wavelength, (b) a short-term temporal stability measurement (30 min), and (c) spectral radiance and temperature measurements at the center of the UUT. After these measurements are completed, the effective emissivity can be calculated using the measured spectral radiance, the known background temperature values, and the set-point temperature (as a reference temperature). We have implemented a two-dimensional linear interpolation that allows the customer to predict the effective emissivity, the apparent radiance, and the radiance temperature for any given temperature set point and background temperature. These values are computed with the user-specified wavelength step within the following spectral bands only: 3.2–4.2 μm , 4.4–5.4 μm , and 8–13.5 μm . The stated uncertainty is only applicable to the ambient background temperature(s) as shown in the characterization certificate. Other values can be used for estimation purposes only.

3.2 Results

Due to limited space, we cannot illustrate the customer BB calibration procedure with a full set of experimental data. Instead, we show an example of experimentally obtained data for a high-temperature flat-plate blackbody. In Fig. 13, we show the anticipated

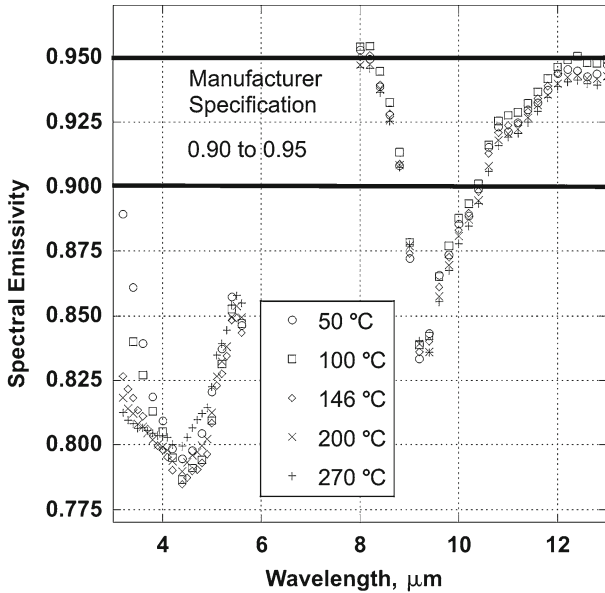


Fig. 14 Effective spectral directional emissivity of a high-temperature flat-plate BB. Manufacturer specification is 0.95 (+0.00, −0.05)

and actual radiance temperatures of a high-temperature flat-plate blackbody. The open symbols denote the anticipated radiance temperatures calculated using the set-point (SP) temperature, a nominal emissivity of 0.95, and a background temperature of 24°C. The filled symbols denote measured values. As can be seen from this plot, use of this blackbody relying only on the manufacturer data specification of emissivity at 0.95 (+0.00, −0.05) could easily result in an error up to 20°C, especially in the 3–5 μm range and near 9 μm. At the same time, analysis of the effective spectral directional emissivity (as shown in Fig. 14) indicates a consistent temperature calibration of the surface temperature, because over a wide temperature range only a negligible shift in the calculated emissivity data is observable.

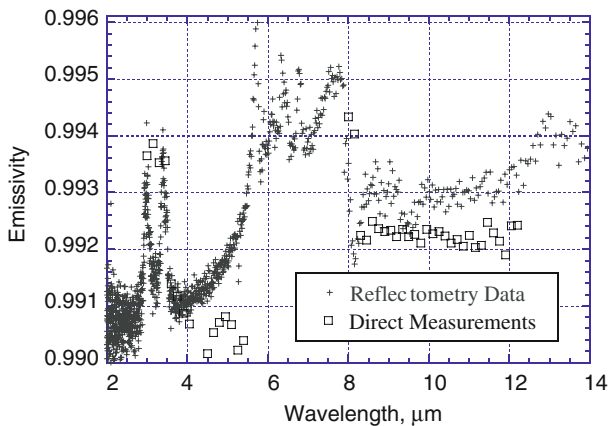
Results of the current uncertainty budget evaluation for the secondary standard BB calibrations are shown in Table 2. We are working at different ways to validate this uncertainty evaluation, including comparisons with other national laboratories, etc. One of these efforts involved comparison of the experimental effective emissivity data for a commercial high-quality flat-plate BB with an indirect emissivity measurement of the coating performed using an IR sphere reflectometer. Results shown in Fig. 15 agree to within 0.1%, which is within the combined uncertainty of the two measurements.

4 Discussion

A systematic realization of IR spectral radiance and radiance temperature scales has been performed. A redundant set of standard blackbody sources with overlapping temperature ranges, differing principles of operation, and different cavity geometries was

Table 2 Uncertainty budget of the measurements of spectral emissivity for the secondary standard BB

Temperature (°C)	Relative expanded uncertainties ($k = 2$) at different wavelength bands ($\times 10^{-3}\text{°C}$)	
	3.4–4.2 μm and 4.4–5.4 μm	8–13 μm
–50	TBD	TBD
10	40	30
30	30	20
70	40	30
150	50	40
250	70	70

**Fig. 15** Comparison of BB emissivity obtained via radiometric (background-corrected) and spectrophotometric measurements

characterized, internally compared, and found to be consistent. An uncertainty budget for scale realization was established, except for the temperature range below 10°C, where further efforts are necessary to independently validate the scale uncertainty.

The implemented capabilities of the AIRI facility for customer IR source calibration include characterization of the absolute spectral radiance and radiance temperature across the spectral range of 3–13 μm and temperature range of 10–250°C with a full calibration uncertainty of 20–70 mK ($k = 2$) and equivalent values for spectral radiance, characterization of the spatial uniformity and stability, and background radiation correction and emissivity (reflectance) evaluation for flat-plate calibrators with emissivities of 0.8 or greater. The NIST-developed spectral comparator TFC provides comparisons in spectrally resolved radiance throughout the temperature range of –50–250°C and over a spectral range of 3–13 μm at the level of 10–50 mK ($k = 2$), depending on the temperature, with a relative spectral resolution of 2–3%. Further efforts are required to fully understand the uncertainties of calibrating targets with high spectral selectivity, low emissivity, and a non-diffuse coating.

For IR imagers and pyrometers, new services include radiance temperature calibrations across the above temperature range, as well as spatial scatter (commonly known as size-of-source effect or SSE) evaluation, essential for correct application of calibration data for different source geometries and backgrounds.

Finally, examples of blackbody calibrations demonstrate the practical significance of the newly established calibration services.

Acknowledgments The authors would like to acknowledge the help of George Eppeldauer and Bob Saunders in the design and characterization of the TFC radiometer; Joel Fowler for engineering assistance; Toni Litorja, Alexander Prokhorov, and Jinan Zeng for coating, modeling, and measuring the BB cavities, respectively; Mart Noorma and Claus Cagran for measurements; and Alex Gura for programming. This project was funded in part by the US Navy.

References

1. J.H. Walker, R.D. Saunders, A.T. Hattenburg, Spectral Radiance Calibrations. NBS Spec. Publ. 250–1 (1987)
2. C.E. Gibson, B.K. Tsai, A.C. Parr, Radiance Temperature Calibrations. NIST Spec. Pub. 250–243 (1998)
3. J.B. Fowler, J. Res. NIST **100**, 591 (1995)
4. J.P. Rice, B.C. Johnson, Metrologia **35**, 505 (1998)
5. B.K. Tsai, J.P. Rice, in *Proceedings of TEMPMEKO 2004, 9th International Symposium on Temperature and Thermal Measurements in Industry and Science*, ed. by D. Zvizdić, L.G. Bermanec, T. Veliki, T. Stašić (FSB/LPM, Zagreb, Croatia, 2004), pp. 859–865
6. J.A. Dykema, J.G. Anderson, Metrologia **43**, 287 (2006)
7. R. Highland, D. Albright, D. Pudlo, T. Robinson Jr., J. Hobbs, EO3: Tester for Emerging Electro-Optical Systems. IEEE Systems Readiness Technology Conference Autotestcon 2005, 223–229 (2005)
8. L.M. Hanssen, S.N. Mekhontsev, V.B. Khromchenko, Infrared spectral emissivity characterization facility at NIST. Proc. SPIE **5405**, 1 (2004)
9. S.N. Mekhontsev, M. Noorma, A.V. Prokhorov, L.M. Hanssen, IR spectral characterization of customer blackbody sources: first calibration results. Proc. SPIE **6205**, 620503 (2006)
10. M. Ballico, Metrologia **37**, 295 (2000)
11. S. Clausen, in *Proceedings of TEMPMEKO 2001, 8th International Symposium on Temperature and Thermal Measurements in Industry and Science*, ed. by B. Fellmuth, J. Seidel, G. Scholz (VDE Verlag, Berlin, 2002), pp. 259–264
12. F.A. Best, H.E. Revercomb, G.E. Bingham, R.O. Knuteson, D.C. Tobin, D.D. LaPorte, W.L. Smith, Calibration of the Geostationary Imaging Fourier Transform Spectrometer (GIFTS). Proc. SPIE **4151**, 21 (2001)
13. A.L. Reesink, N.L. Rowell, A.G. Steele, Using Fourier- Transform Blackbody Spectra to Determine Thermodynamic Temperature in the 600°C to 1000°C Range. in *Temperature: Its Measurement and Control in Science and Industry*, vol. 7, ed. by D.C. Ripple (AIP, New York, 2003), pp. 19–34
14. L.M. Hanssen, S.N. Mekhontsev, J. Zeng, A.V. Prokhorov, in *Proceedings of TEMPMEKO 2007*, Int. J. Thermophys., doi: [10.1007/s10765-007-0314-8](https://doi.org/10.1007/s10765-007-0314-8)
15. A.V. Prokhorov, Metrologia **35**, 465 (1998)
16. V.B. Khromchenko, S.N. Mekhontsev, L.M. Hanssen, Design and Evaluation of Large Aperture Galvanic Fixed Point Blackbody. in *Proceedings of TEMPMEKO 2007* (to be published in Int. J. Thermophys.)
17. Certain commercial equipment, instruments, or materials are identified in this article to specify the experimental procedure adequately. Such identification is not intended to imply recommendation or endorsement by the National Institute of Standards and Technology, nor is it intended to imply that the materials or equipment identified are necessarily the best available for the purpose
18. B. Chu, G. Machin, Meas. Sci. Technol. **10**, 1 (1999)

19. M. Noorma, S.N. Mekhontsev, V.B. Khromchenko, J. Envall, and L.M. Hanssen, Study of Water Heat Pipe Blackbody as a Standard for Infrared Spectral Radiance and Radiance Temperature. in *Proceedings of TEMPMEKO 2007* (to be published in Int. J. Thermophys.)
20. M. Noorma, S. Mekhontsev, V. Khromchenko, A. Gura, M. Litorja, B. Tsai, L.M. Hanssen, Design and Characterization of Si and InGaAs Pyrometers for Radiance Temperature Scale Realization between 232°C and 962°C. Proc. SPIE **6205**, 620501 (2006)
21. J. Envall, S.N. Mekhontsev, Y. Zong, L.M. Hanssen, Spatial Scatter Effects in the Calibration of IR Pyrometers and Imagers. in *Proceedings of TEMPMEKO 2007* (to be published in Int. J. Thermophys.)